

## Original Research Article

# Calycosin regulates glucocorticoid-induced apoptosis via Nrf2/ARE signaling in MC3T3-E1 cells

Lifeng Fu<sup>1</sup>, WeiLiang Wu<sup>2</sup>, Jian Zhu<sup>2</sup>, Shu Qiang<sup>2</sup>, Jansong Chen<sup>2\*</sup>

<sup>1</sup>Department of Orthopaedics, Hospital of Traditional Chinese Medicine, Keqiao District, Shaoxing, Zhejiang 312030,

<sup>2</sup>Department of Orthopaedics, Children's Hospital, School of Medicine, Zhejiang University, Zhejiang 310000, PR China

\*For correspondence: **Email:** [jsongchen@163.com](mailto:jsongchen@163.com)

Sent for review: 18 October 2017

Revised accepted: 12 January 2018

### Abstract

**Purpose:** To determine the anti-osteoporotic effect of calycosin (CA) and investigate the mechanism involved.

**Methods:** To establish a cell model of osteoporosis, MC3T3-E1 cells were treated with dexamethasone (DEX). Subsequently, the levels of accumulated reactive oxygen species (ROS) and subsequent apoptotic cell death (using flow cytometry) were determined. Relevant mRNA and protein expression levels were measured by quantitative reverse transcription polymerase chain reaction (qRT-PCR) and immunoblot respectively.

**Results:** CA reduced the apoptosis and accumulation of ROS in DEX-treated cells. DEX induced the expression of caspase-3/-8/-9 in the cleavage of poly ADP-ribose polymerase (PARP), whereas CA treatment decreased expression levels of caspase-3/-8/-9 and PARP. In addition, DEX treatment significantly suppressed the expression of nuclear factor-erythroid 2-related factor 2 (Nrf2) as well as its downstream targets, viz, heme oxygenase-1 and quinone oxidoreductase-1. Interestingly, CA treatment reversed this suppressive effect. It was also found that Nrf2 small interfering RNA effectively inhibited the protective effects of CA against DEX-induced ROS overproduction as well as apoptosis.

**Conclusion:** CA attenuates the cytotoxicity of DEX via inhibition of the generation of ROS and promotion of Nrf2 expression. These findings offer novel insights into a molecular approach to the treatment of glucocorticoid-induced osteoporosis via the application of natural compounds.

**Keywords:** Calycosin, Osteoporosis, Nrf2, Antioxidant response elements, Apoptosis

This is an Open Access article that uses a funding model which does not charge readers or their institutions for access and distributed under the terms of the Creative Commons Attribution License (<http://creativecommons.org/licenses/by/4.0>) and the Budapest Open Access Initiative (<http://www.budapestopenaccessinitiative.org/read>), which permit unrestricted use, distribution, and reproduction in any medium, provided the original work is properly credited.

Tropical Journal of Pharmaceutical Research is indexed by Science Citation Index (SciSearch), Scopus, International Pharmaceutical Abstract, Chemical Abstracts, Embase, Index Copernicus, EBSCO, African Index Medicus, JournalSeek, Journal Citation Reports/Science Edition, Directory of Open Access Journals (DOAJ), African Journal Online, Bioline International, Open-J-Gate and Pharmacy Abstracts

## INTRODUCTION

Osteoporosis is a threat to health, particularly in postmenopausal women [1]. Osteoporosis is characterized by imbalance in the processes of bone formation and resorption, resulting in

degenerative bone mineral density and deteriorative bone microarchitecture, which eventually lead to loss of bone strength and an increased risk of fracture [2]. Normal process of bone metabolism largely rely on the dynamic equilibrium between bone formation and bone

resorption. Osteoclasts and osteoblasts have been reported to play a vital role in maintaining normal bone mass in bony remodeling [3]. The destruction of osteoblasts causes reduced bone formation and imbalanced bone metabolism. Glucocorticoids (GCs) are known to induce osteoporosis, primarily by suppressing osteoblast-mediated osteogenesis [4,5]. In this research, a cell model of osteoporosis was established by treating osteoblasts with a synthetic GC dexamethasone (DEX).

Calycosin (CA) is a compound isolated from *Radix astragali* (Figure 1), referred as *Huangqi* in Chinese, which is widely used in traditional medicine in China. In traditional Chinese medicine, Qi is involved in vital substances that contribute to the physiological functions of organs and meridians. Specifically, *Huangqi* has been widely used to tonify Qi [6-8] and is reported to have a protective effect in postmenopausal women who suffer from osteoporosis [9]. Additionally, total flavones of astragalus extract have also been shown to increase the BMD of ovariectomized rats [10]. However, the effect of CA, which is one of the flavones in *Radix astragali*, on osteoporosis remains unclear. Therefore, the aim of the present study was to investigate the therapeutic effect of CA in bone loss-associated diseases in post-menopausal women.

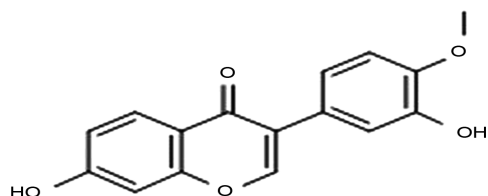


**Figure 1:** Chemical structure of calycosin

## EXPERIMENTAL

### Cell culture

MC3T3-E1 osteoblastic cell line (Shanghai Cell Bank, Chinese Academy of Sciences) was cultured in  $\alpha$ -Modified Eagle's Medium (MEM) (Gibco, USA), supplemented with 10% fetal bovine serum (Thermo Fisher Scientific, USA) at 37 °C in a 5 % CO<sub>2</sub> humidified atmosphere.

### Assessment of cell viability

To study the potential effects of CA on MC3T3-E1 cells, different concentrations of CA (20 and 80  $\mu$ M) were used to pre-treat the cells ( $1 \times 10^5$  cells/cm<sup>2</sup>) for 2 hrs at 37 °C. Subsequently, DEX (10  $\mu$ M, Sigma-Aldrich, USA) was mixed with the culture medium and incubated for 24 hrs. A Cell

Counting Kit (CCK)-8 kit (beyotime, China) was utilized to measure the cell viability described by Huang *et al* [11]. Then,  $4 \times 10^3$  cells were dispersed in each well of a 96-well plate and cultured for 6, 12, 24 and 48 hrs respectively. Each well was dispersed with CCK-8 reagent 1 h prior to the incubation. Then, a microplate reader (BD Biosciences, USA) was utilized to measure the optical density at 450 nm wavelength. All the parallel experiments were repeated for >3 times.

### Measurement of apoptosis frequency

The apoptosis rate of cells were evaluated using an Annexin V-FITC apoptosis detection kit (KeyGEN Biotech, China). MC3T3-E1 cells were harvested after treatment of DEX for 24 hrs, the mixture was washed with ice-cold 1xPBS buffer and re-suspended in 500 $\mu$ L binding buffer. After addition of 5  $\mu$ L Annexin V stock solution, the mixture was incubated at 4 °C for 10 min. FACSCalibur flow cytometer (BD Biosciences, USA) was utilized to analyze immediately following the addition of 5  $\mu$ L propidium iodide.

### Determination of ROS

Flow cytometric analysis was applied to detect ROS levels in cells as described previously [12]. After incubating with dihydrorhodamine 123 (0.5  $\mu$ M; Sigma-Aldrich, USA) at 37 °C for 0.5 hrs, the MC3T3-E1 cells were washed with 1xPBS and re-suspended in complete medium. After this treatment, the fluorescent intensity was assessed by a flow cytometry (Ex, 490 nm; Em, 520 nm).

### qRT-PCR analysis

TRIzol reagent (Gibco; Thermo Fisher Scientific) was utilized to separate Total RNA from the cells. RT-qPCR analysis was completed on an ABI 7500 thermal cycler (Applied Biosystems), and 20 ng template RNA was used in a 25  $\mu$ L reaction volume with 2x SYBR<sup>®</sup> Green PCR Master mix (Thermo Fisher Scientific, USA) and gene specific primer pairs. cDNA was synthesized at 55 °C for 30 min following manufacture's protocol. qRT-PCR cycles were stated in Table 1.  $2^{-\Delta\Delta Ct}$  value was adopted to quantify relative mRNA expression levels of the target genes, compared to GAPDH [13].

**Table 1:** qRT-PCR cycle

Variable	Temperature (°C)	Time	Cycle
Pre-denaturation	94	2 min	1
Denaturation	94	15 s	40
Annealing	60	30 s	
Extension	68	50 s	
Extension	68	5 min	1

**Table 2:** Primers for RT-qPCR analysis

Variable	Forward	Reverse	Product length
Nfr2	5'- TTCCTCTGCTGCCATTAG TCAGTC-3'	5'- GCTCTTCCATTTCCGAGTCA CTG-3'	215 bps
Heme oxygenase-1 (HO1)	5'- ATCGTGCTCGCATGAAC ACT-3'	5'CCAACACTGCATTTACATG GC-3'	339 bps
NAD(P) H: quinone oxidoreductase-1 (NQO1)	5'- ACTCGGAGAACTTTTCAGT ACC-3'	5'- TTGGAGCAAAGTAGAGTGG T-3'	492 bps
GAPDH	5'- ATCACTGCCACCCAGAA G-3'	5'- TCCACGACGGACACATTG-3'	191 bps

### Immunoblot analysis

Cells were washed twice with 1xPBS buffer, then lysed in RIPA buffer (Beyotime, China) containing 1 % protease inhibitor cocktail (PIC) (Sigma-Aldrich, USA). The supernatant of the cell lysates was collected, and the protein concentrations were measured via BCA assay (Thermo Fisher Scientific, USA). Proteins (20-30 µg) were separated by 10 - 12 % SDS-polyacrylamide gels, which were transferred onto polyvinylidene fluoride membranes (Millipore, USA). After blocking, membranes were incubated with primary antibodies including anti-caspases -3, -8, and -9 (1:1000; catalog nos. ab2171, ab25901 and ab52298; Abcam, UK), anti-PARP (1:1000; catalog no. ab4830; Abcam, UK), anti-Nrf2 (1:1000; catalog no. PA5-19830; Invitrogen, USA), anti-HO1 (1:1000; catalog no. MA1-112; Invitrogen, USA), anti-NQO1 (1:1000; catalog no. 39-3700; Invitrogen, USA), and anti-GAPDH (1:1500; catalog no. MA5-15738; Invitrogen, USA) for 1 h at room temperature. After wash with 1xPBS buffer, membranes were subsequently incubated with goat anti-mouse (catalog no. A23610) or goat anti-rabbit (catalog no. A23620) secondary HRP antibody (1:1000; Beyotime, China) for 45 min at 22 °C. Bands were developed using enhanced chemiluminescence (ECL) (Thermo Fisher Scientific, USA) and quantified by densitometry analysis of Quantity One® 1-D Analysis software (V. 4.6.8; Bio-Rad, USA).

### RNA interference

To achieve a confluence of 60 - 80 % confluence,  $2 \times 10^5$  MC3T3-E1 cells per well were seeded and cultured overnight. The silencing assay was performed according to manufacturer's protocol, with a Nrf2 small interfering (si) RNA assay kit that contained a pool of three 19-25 nucleotide target-specific Nrf2 siRNAs (catalog no. sc-37049; Santa Cruz Biotechnology, USA). Expression levels of Nrf2

and its downstream targets, i.e., HO1 and NQO1, were measured using immunoblot analysis.

### Statistical analysis

SPSS (version 16.0, IBM, USA) was applied to analyze the experimental results. One-way analysis of variance (ANOVA) was performed. Type of post-hoc test is dependent on whether the variances are homogeneous (LSD) or heterogeneous (Dunnnett T3). Statistical significant difference was set at a threshold of  $p < 0.05$ .

## RESULTS

### Effect of CA on cell viability

To investigate the effects of CA on cell proliferation, a CCK-8 assay was performed (Figure 2). We observed that  $>20 \mu\text{M}$  doses of CA significantly increased the viability of the MC3T3-E1 cells at 6, 12, 24, and 48 hrs (Figure 2A). In addition, CA promoted cell proliferation in a dose- and time-dependent way. Hence, 20 and 80 µM doses of CA were used in the following studies.

### Effect of CA on the DEX-induced apoptosis

To investigate effects of CA on apoptosis, DEX-treated cells were treated with CA. The results demonstrated that cells viability was significantly suppressed by DEX compared to the untreated group. However, CA significantly increased the viability of the DEX-treated cells in a dose- and time-dependent way (Figure 2 B). Moreover, apoptotic rates of the cells in the control, DEX, CA 20 µM and CA 80 µM groups were also measured (Figure 3 A). Treatment with DEX lead to an apoptotic frequency of 36.42 %, compared to 6.84 % in the control group. However, CA decreased the apoptotic frequency to 28.26 (20 µM) and 14.35 % (80 µM). Therefore, CA

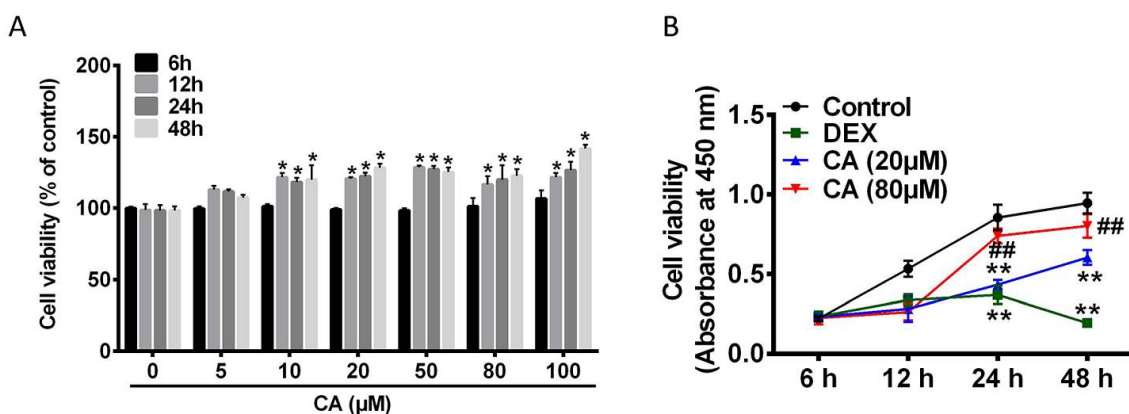


**Figure 2:** Effect of CA on MC3T3-E1 cell viability. (A) Cells were exposed to CA (concentrations at 0, 5, 10, 20, 50, 80, and 100 μM) for 6, 12, 24 and 48 h, then CCK8 assay was used to ascertain the cell viability. (B) Different doses of CA (0, 20 and 80 μM) were used to treat the cells for 2 h. Treated cells were then exposed to DEX for 24 h. Cell viability was quantified by a CCK8 assay. (Error bar: mean ± SD; n = 6; ##  $p < 0.01$ , vs. the untreated group; \*  $p < 0.05$ , \*\*  $p < 0.01$ , vs. the DEX-treated group). Abbreviations: CA, calycosin; DEX, dexamethasone

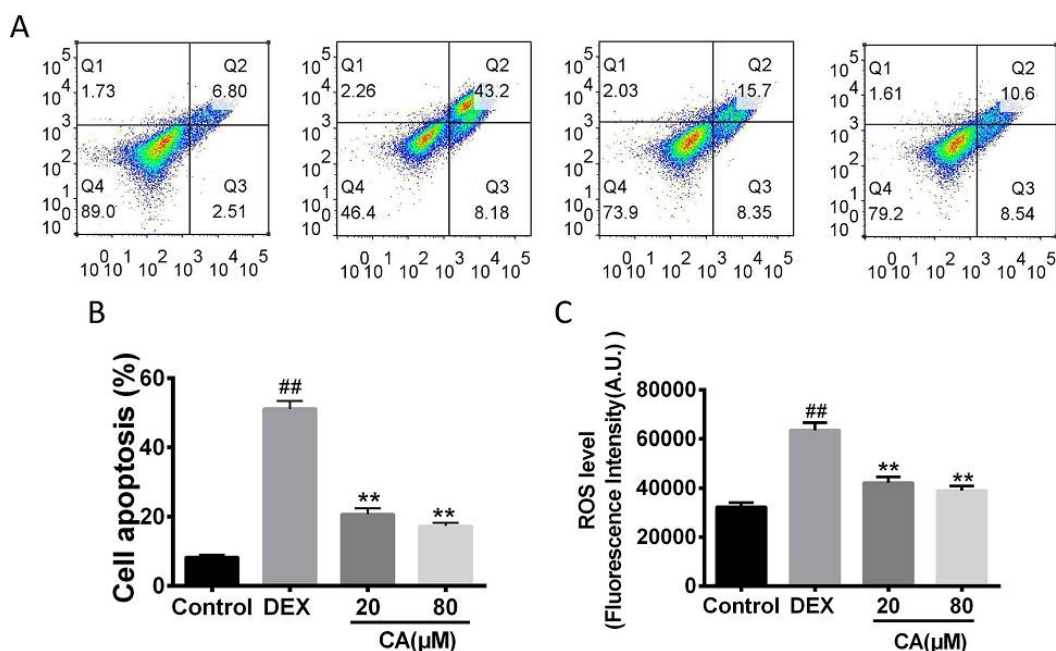


**Figure 3:** Effects of CA on ROS and apoptotic levels in DEX-treated cells. (A) Cells were treated with series of doses of CA (0, 20 and 80 μM) for 2 h, followed by 24 h DEX exposure. Apoptosis was measured using Annexin V assay. (B) ROS levels, determined by flow cytometry. (Error Bar: mean ± SD; n = 6; ##  $p < 0.01$ , vs. the untreated group; \*  $p < 0.05$ , \*\*  $p < 0.01$ , vs. the DEX-treated group). Abbreviation: CA, calycosin; DEX, dexamethasone

exhibited a protective effect against apoptosis upon DEX treatment.

#### Effect of CA on ROS production following DEX treatment

As shown in Figure 3 C, ROS levels were significantly increased following 24 h of DEX treatment, as compared to control group levels. However, treatment with 20 and 80 μM CA effectively reduced the higher ROS level observed in the DEX-treated group.

#### Effect of CA on caspase-3/-8/-9 and PARP expression levels

The immunoblot analysis showed the levels of caspase-3/-8/-9 increased dramatically in DEX treated MC3T3-E1 cells (Figure 4 A-B), suggesting DEX-induced apoptosis was mediated by mitochondria and/or death receptor. However, CA treatment (20 and 80 μM) significantly suppressed the DEX-induced activation and upregulation of caspases (-3, -8 and -9) in a dose-dependent way of the inhibition occurred simultaneously. In addition, DEX treatment resulted in PARP cleavage (Figure 4).

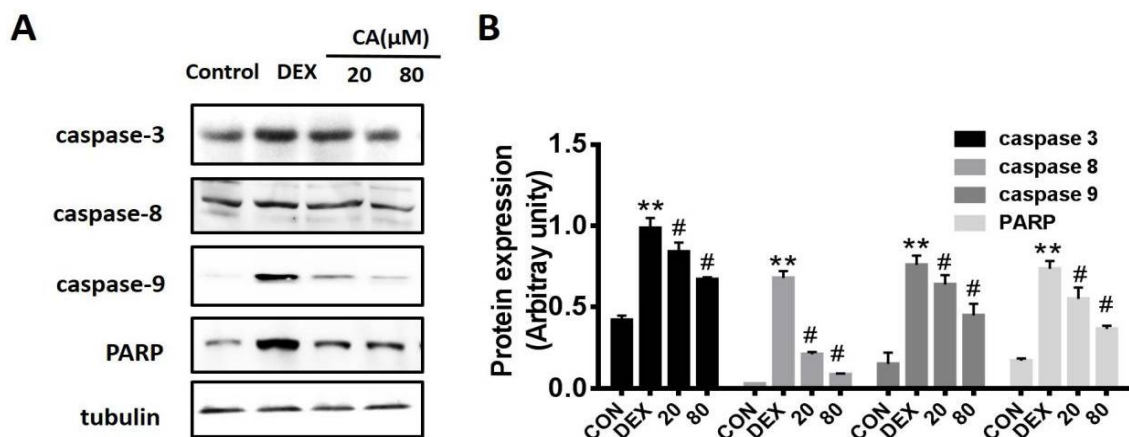


**Figure 4:** Effect of CA on caspase-3/-8/-9 and PARP expression levels. Cells were treated with different doses of CA (0, 20 and 80  $\mu$ M) for 2 h, followed by 12 h of DEX exposure. (A) Caspase-3/-8/-9 and PARP expression levels were quantified using immunoblot. (B) Quantification of the Western blot results. (Error Bar: mean  $\pm$  SD; n = 6; ## $p$  < 0.01, vs. the untreated group; \*\* $p$  < 0.01, vs. the DEX-treated group). Abbreviation: CA, calycosin; DEX, dexamethasone. PARP, poly (ADP-ribose) polymerase

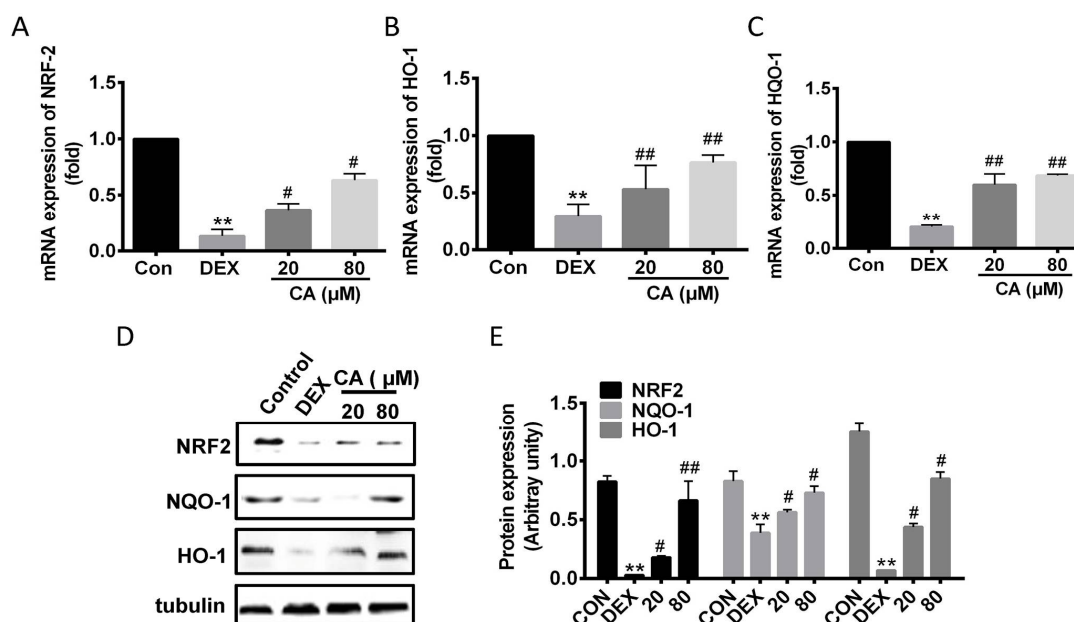


**Figure 5:** Effect of CA on Nrf2 and its downstream targets. Levels of mRNA expression of (A) Nrf2, (B) NQO1 and (C) HO1. (D) Protein expression levels of Nrf2, NQO1 and HO1. (E) Quantification of protein expression. (Error Bar: mean  $\pm$  SD; n = 6; ## $p$  < 0.01, vs. the untreated group; \*\* $p$  < 0.01, vs. the DEX-treated group). Abbreviation: CA, calycosin; DEX, dexamethasone

As expected, this cleavage was suppressed by the addition of CA (20 and 80  $\mu$ M). Taken together, the results demonstrated that CA inhibited apoptosis in osteoblastic cells.

### Effect of CA on Nrf2 signaling

The RT-qPCR and western blot showed DEX treatment suppressed mRNA levels of Nrf2 and its downstream effectors (Figure 5 A-C). However, CA reversed this decrease. As shown in Figure 5 D and E, the expression levels of Nrf2, HO1 and NQO1 were significantly suppressed in DEX-treated MC3T3-E1 cells.

After CA treatment, Nrf2, HO1, and NQO1 expression was effectively recovered, suggesting that CA inhibited the DEX-induced ROS production via Nrf2 signaling activation.

### Involvement of Nrf2 pathway in the interactions of DEX and CA

As the results shown in Figure 6A, Nrf2-siRNA downregulated levels of Nrf2, HO1 and NQO1, demonstrating Nrf2 silencing was effective. The effects on apoptosis of DEX-induced cell arising from Nrf2-knockdown were also examined. As shown in Figure 6 A-B, CA reduced DEX-induced

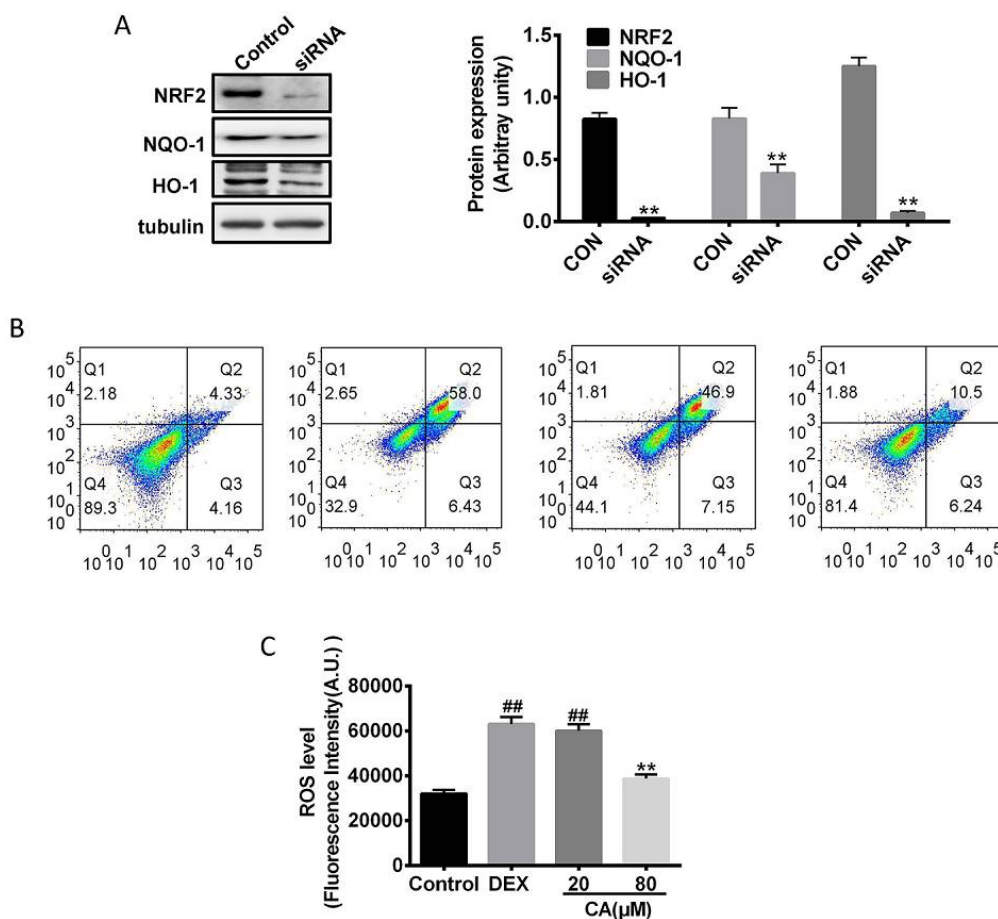


**Figure 6:** Effect of CA on Nrf2 signaling. (A) Protein levels of Nrf2, HO1 and NQO1 after treatment with siRNA-Nrf2 for 24 h. Effect of CA on apoptosis (B) and ROS levels (C). (Error Bar: mean  $\pm$  SD; n = 6; ##*p* < 0.01, vs. the untreated group; \*\**p* < 0.01, vs. the DEX-treated group). Abbreviation: CA, calycosin; DEX, dexamethasone

apoptosis that resulted from ROS overproduction. In addition, Nrf2-siRNA inhibited the protective effects of CA. Thus, Nrf2 knockdown recovered the DEX-induced cytotoxicity. Supplementation of CA reversed the DEX-induced cell apoptosis from 31 to 11.6 %. However, Nrf2 siRNA increased the apoptotic rate of MC3T3-E1 cells to 23.7 %. CA reduced the DEX-induced ROS overproduction from 212 % in the control to 119 %, showing a recovery of 93 % (Figure 6C).

## DISCUSSION

CA, a phytoestrogen, is a major active flavonoid in *Radix Astragali* [14,15], which shows antitumor, antioxidative and anti-osteoporotic abilities [6]. It is reported that calycosin-7-O- $\beta$ -D-glucopyranoside inhibits osteoclast development *in vitro* and bone loss *in vivo*. Through regulating the bone morphogenetic protein/WNT signaling pathways, calycosin-7-O- $\beta$ -D-glucopyranoside can also promote the osteoblastic cell differentiation in ST2 model (16). CA also exerts a protective role in bone loss in ovariectomized rats in a dose-dependent way [17]. Here, we

explored the effects of CA on MC3T3-E1 cells upon DEX treatment, a synthetic GC. Our research revealed that CA promoted cell proliferation in a dose-/time-dependent way. In the DEX-treated cells, CA decreased the apoptosis rate and intracellular levels of ROS. Collectively, CA exhibited protective effects on the DEX-treated MC3T3-E1 cells.

Generation of ROS can cause loss of mitochondrial membrane potential, which ultimately resulting in cell apoptosis. Our data illustrated that the supplementation of CA effectively inhibited the rapid onset and time-dependent production of ROS, which is induced by DEX. Our findings demonstrated that CA protected MC3T3-E1 cells from cytotoxicity via inhibiting ROS production. The study also demonstrated downstream effects caused by increased ROS production in osteoblastic cells. Functioning as one of the major regulators of cytoprotective responses, the Nrf2 signaling pathway responds to changes in ROS and electrophiles that are associated with endogenous and exogenous stress [18,19]. Therefore, western blot and qRT-PCR analyses

are useful methods for determining the effects of DEX treatment on Nrf2 and its downstream genes. These results illustrated that mRNA levels of Nrf2, HO1 and NQO1 were decreased in the DEX-treated MC3T3-E cells. To examine the role of Nrf2 signaling in DEX-induced apoptotic cell death, we analyzed the ability of DEX to induce and the ability of CA to protect against apoptosis using Nrf2-siRNA. The results showed that CA protected against DEX-induced apoptosis and increased ROS levels. These protective effects were significantly decreased by downregulation of Nrf2.

## CONCLUSION

The findings of this study demonstrate that ROS-mediated downregulation of Nrf2 contributes to DEX-induced cytotoxicity in MC3T3-E1 osteoblastic cells, and that CA reverses DEX-cytotoxicity by inhibiting the accumulation of ROS and promoting the expression of Nrf2. These results provide an insight into potential molecular treatment strategies for DEX-induced osteoporosis using natural compounds.

## DECLARATIONS

### Conflict of Interest

No conflict of interest associated with this work.

### Contribution of Authors

The authors declare that this work was done by the authors named in this article and all liabilities pertaining to claims relating to the content of this article will be borne by them. Lifeng wrote this paper and participated in the study design and experiments, Wei Liang Jian and Zhu Wu performed the experiments and analyzed the data, Jansong Chen and Shu Qiang designed this study and supervised the experiments.

## REFERENCES

1. Tanaka Y, Mori H, Aoki T, Atsumi T, Kawahito Y, Nakayama H, Tohma S, Yamanishi Y, Hasegawa H, Tanimura K, et al. Analysis of bone metabolism during early stage and clinical benefits of early intervention with alendronate in patients with systemic rheumatic diseases treated with high-dose glucocorticoid: Early Diagnosis and Treatment of Osteoporosis in Japan (EDITOR-J) study. *J Bone Miner Metab* 2016; 34: 646.
2. McCloskey E. A BMD threshold for treatment efficacy in osteoporosis? A need to consider the whole evidence base. *Osteoporos Int* 2016; 27(1): 417-419.
3. Rosario PW, Carvalho M, Calsolari MR. Symptoms of Thyrotoxicosis, Bone Metabolism, and Occult Atrial Fibrillation in Older Women with Mild Endogenous Subclinical Hyperthyroidism. *Clin Endocrinol (Oxf)* 2015; 85(1): 132-136.
4. Yao W, Cheng Z, Busse C, Pham A, Nakamura MC, Lane NE. Glucocorticoid excess in mice results in early activation of osteoclastogenesis and adipogenesis and prolonged suppression of osteogenesis: a longitudinal study of gene expression in bone tissue from glucocorticoid-treated mice. *Arthritis Rheum* 2008; 58: 1674-1686.
5. Phillips JE, Gersbach CA, Wojtowicz AM, Garcia AJ. Glucocorticoid-induced osteogenesis is negatively regulated by Runx2/Cbfa1 serine phosphorylation. *J Cell Sci* 2006; 119: 581-591.
6. Qiu R, Ma G, Zheng C, Qiu X, Li X, Li X, Mo J, Li Z, Liu Y, Mo L, et al. Antineoplastic effect of calycosin on osteosarcoma through inducing apoptosis showing in vitro and in vivo investigations. *Exp Mol Pathol* 2014, 97(1): 17-22.
7. Zhou Y, Liu QH, Liu CL, Lin L. Calycosin induces apoptosis in human ovarian cancer SKOV3 cells by activating caspases and Bcl-2 family proteins. *Tumour Biol* 2015; 36: 5333-5339.
8. Wu J, Xu H, Zhang L, Zhang X. Radix Astragali and Tanshinone Help Carboplatin Inhibit B16 Tumor Cell Growth. *Technol Cancer Res Treat* 2015; 15(4): 583-588.
9. Guo CC, LH Zheng, Fu JY, Zhu JH, Zhou YX, Zeng T, Zhou ZK. Antiosteoporotic Effects of Huangqi Sanxian Decoction in Cultured Rat Osteoblasts by Proteomic Characterization of the Target and Mechanism. *Evid-Based Compl Alt* 2015; (1): 1-10.
10. Cao J, Chen Z, Zhu Y, Li Y, Guo C, Gao K, Chen L, Shi X, Zhang X, Yang Z, et al. Huangqi-Honghua combination and its main components ameliorate cerebral infarction with Qi deficiency and blood stasis syndrome by antioxidant action in rats. *J Ethnopharmacol* 2014; 155: 1053-1060.
11. Huang J, Sun C, Wang S, He Q, Li D. microRNA miR-10b inhibition reduces cell proliferation and promotes apoptosis in non-small cell lung cancer (NSCLC) cells. *Mol Biosyst* 2015; 11: 2051-2059.
12. Chen JY, Zhang L, Zhang H, Su L, Qin LP. Triggering of p38 MAPK and JNK signaling is important for oleanolic acid-induced apoptosis via the mitochondrial death pathway in hypertrophic scar fibroblasts. *Phytother Res* 2014; 28: 1468-1478.
13. Livak KJ, Schmittgen TD. Analysis of relative gene expression data using real-time quantitative PCR and the 2- $\Delta\Delta$ CT method. *Methods* 2001; 25: 402-408.
14. Zhao XL, Liu L, Di LQ, Li JS, Kang A. Studies on effects of calycosin-7-O-beta-D-glucoside on prim-O-glucosylcimifugin and cimifugin in vivo pharmacokinetics. *Zhongguo Zhong Yao Za Zhi* 2014; 39: 4669-4674.

15. Ruan JQ, Yan R. Regioselective glucuronidation of the isoflavone calycosin by human liver microsomes and recombinant human UDP-glucuronosyltransferases. *Chem Biol Interact* 2014; 220: 231-240.
16. Jian J, Sun L, Cheng X, Hu X, Liang J, Chen Y. Calycosin-7---d-glucopyranoside stimulates osteoblast differentiation through regulating the BMP/WNT signaling pathways. *Acta Pharm Sin B* 2015; 5: 454-460.
17. Hong W. Experimental study on the effect of Calycosin on prevention and treatment of osteoporosis in ovariectomized rats. *Orthop Biomech Mater Clin Study* 2010; 07: 11-14.
18. Roy CS, Sengupta S, Biswas S, Sinha TK, Sen R, Basak RK, Adhikari B, Bhattacharyya A. Bacterial fucose-rich polysaccharide stabilizes MAPK-mediated Nrf2/Keap1 signaling by directly scavenging reactive oxygen species during hydrogen peroxide-induced apoptosis of human lung fibroblast cells. *Plos One* 9: e113663, 2014.
19. McMahon M, Campbell KH, MacLeod AK, McLaughlin LA, Henderson CJ, Wolf CR. HDAC inhibitors increase NRF2-signaling in tumour cells and blunt the efficacy of co-administered cytotoxic agents. *Plos One* 2014; 9: e114055.